References

ALEANDRI, L. E. & MCCARLEY, R. E. (1988). *Inorg. Chem.* **27**, 1041–1044.

B. A. FRENZ & ASSOCIATES INC. (1982). *SDP Structure Determination Package*. College Station, Texas, USA.

BART, J. C. & RAGAINI, V. (1979). *Inorg. Chim. Acta*, **36**, 261–265.

BETTERIDGE, P. W., CHEETHAM, A. K., HOWARD, J. A. K., JAKUBICKI, G. & MCCARROLL, W. H. (1984). *Inorg. Chem.* **23**, 737–740.

BURSILL, L. A. & GRZINIC, G. (1980). *Acta Cryst.* B**36**, 2902–2913.

CHEARY, R. W. (1990). *Acta Cryst.* B**46**, 599–609.

CHEARY, R. W. & SQUADRITO, R. (1989). *Acta Cryst.* B**45**, 205–212.

FANCHON, E., VICAT, J., HODEAU, J.-L., WOLFERS, P., TRAN QUI, D. & STROBEL, P. (1987). *Acta Cryst.* B**43**, 440–448.

FISCHER, P., HÄLG, W., SCHLAPBACH, L. & YVON, K. (1978). *J. Less-Common Met.* **60**, 1–9.

HAMILTON, W. C. (1965). *Acta Cryst.* **18**, 502–510.

KOMDEUR, A. J. H., DE BOER, J. L. & VAN SMAALEN, S. (1990). *J. Phys. Condens. Matter*, **2**, 45–54.

LELIGNY, H., LEDÉSERT, M., LABBÉ, PH., RAVEAU, B. & MCCARROLL, W. H. (1990). *J. Sold State Chem.* **87**, 35–43.

MCCARLEY, R. E. (1986). *Polyhedron*, **5**, 51–61.

MCCARLEY, R. E., LII, K.-H., EDWARDS, P. A. & BROUGH, L. F. (1985). *J. Solid State Chem.* **57**, 17–24.

MCCARROLL, W. H., DARLING, C. & JAKUBICKI, G. (1983). *J. Solid State Chem.* **48**, 189–195.

MCCARROLL, W. H., KATZ, L. & WARD R. (1957). *J. Am. Chem. Soc.* **79**, 5410–5414.

MIJLHOFF, F. C., IJDO, D. J. W. & ZANDBERGEN, H. W. (1985). *Acta Cryst.* B**41**, 98–101.

POST, J. E., VON DREELE, R. B. & BUSECK, P. R. (1982). *Acta Cryst.* B**38**, 1056–1065.

SINCLAIR, W. & MCLAUGHLIN, G. M. (1982). *Acta Cryst.* B**38**, 245–246.

SINCLAIR, W., MCLAUGHLIN, G. M. & RINGWOOD, A. E. (1980). *Acta Cryst.* B**36**, 2913–2918.

TARASCON, J. (1986). *Solid State Ionics*, **22**, 85–96.

TORARDI, C. C. & CALABRESE, J. C. (1984). *Inorg. Chem.* **23**, 3281–3284.

TORARDI, C. C. & MCCARLEY, R. E. (1981). *J. Solid State Chem.* **37**, 393–397.

TORARDI, C. C. & MCCARLEY, R. E. (1985). *Inorg. Chem.* **24**, 476–481.

TORARDI, C. C. & MCCARLEY, R. E. (1986). *J. Less-Common Met.* **116**, 169–186.

VICAT, J., FANCHON, E., STROBEL, P. & TRAN QUI, D. (1986). *Acta Cryst.* B**42**, 162–167.

WOLFF, P. M. DE (1977). *Acta Cryst.* A**33**, 493–497.

WOLFF, P. M. DE, JANSSEN, T. & JANNER, A. (1981). *Acta Cryst.* A**37**, 625–636.

XIANG, S.-B., FAN, H.-F., WU, X.-J., LI, F.-H. & PAN, Q. (1990). *Acta Cryst.* A**46**, 929–934.

YAMAMOTO, A. (1982). *REMOS*. A computer program for the refinement of modulated structures. National Institute for Research in Inorganic materials, Niiharigun, Ibaraki, Japan.

YAMAMOTO, A., NAKAZAWA, H., KITAMURA, M. & MORIMOTO, N. (1984). *Acta Cryst.* B**40**, 228–237.

Acta Cryst. (1992). B**48**, 144–151

Charge Density Around a Jahn–Teller-Distorted Site: $(ND_4)_2Cu(SO_4)_2.6D_2O$ at 85 K

BY BRIAN N. FIGGIS, LECIA KHOR, EDWARD S. KUCHARSKI AND PHILIP A. REYNOLDS

School of Chemistry, University of Western Australia, Nedlands, WA 6009, *Australia*

(*Received* 6 *August* 1991; *accepted* 5 *November* 1991)

Abstract

Diammonium hexaaquacopper(II) disulfate-d_{20}, $[ND_4]_2[Cu(D_2O)_6](SO_4)_2$, $M_r = 419.7$, monoclinic, $P2_1/a$, $a = 9.399$ (2), $b = 12.673$ (2), $c = 6.071$ (1) Å, $\beta = 107.13$ (1)°, $V = 691.1$ (4) Å^3, $Z = 2$, $D_x = 2.02$ Mg m^{-3}, Mo $K\alpha$ radiation, $\lambda = 0.71069$ Å, $\mu = 2.008$ mm^{-1}, $F(000) = 415.3$, $T = 85$ (2) K, $R(I) = 0.020$, $R(F) = 0.014$ for 7287 reflections. The CuO_6 octahedron has a large Jahn–Teller distortion; Cu—O(8) 2.301 (1), Cu—O(7) 2.010 (1), Cu—O(9) 1.960 (1) Å. It was necessary to use quartic anharmonic thermal parameters at the Cu^{II} site. These modelled potential softening associated with the Jahn–Teller distortions, important even at this temperature. At the ammonium, the sulfate and the hexaaqua-ion sites the charge densities, at this experimental accuracy, can be described by simple valence functions which reflect only local symmetry. Large lower-symmetry densities are not observed; any small such effects are comparable with uncertainties in the treatment of the thermal motion. The valence refinement gave Cu 3*d* populations of $3d_{xy}^{1.58\,(6)}3d_{xz,yz}^{2.12\,(3)}3d_{z^2}^{2.18\,(6)}3d_{x^2-y^2}^{0.82\,(7)}$. This shows the hole expected in $3d_{x^2-y^2}$, modified, taking overlap into account, by a covalent σ acceptance of 0.52 (1) and π back donation of 0.18 (10) e. The rhombic distortion causes $3d_{z^2}/3d_{x^2-y^2}$ mixing corresponding to a $3d_{z^2}$ coefficient of -0.21 (7) in a spin-hole wavefunction. Ionic charges from the model are $Cu(OD_2)_6^{1.7+}$, $ND_4^{0.6+}$ and $SO_4^{1.5-}$. These are more ionic than for the isomorphous Cr^{II} salt, where σ and π charge

0108-7681/92/020144-08$03.00

flows are both to the metal, not opposed as here. Qualitatively these results agree with the conclusions from ESR, NMR and optical spectra.

Introduction

The electronic structures of hexaaquametal(II) ions are of archetypal importance in understanding metal–ligand bonding. A direct route of study is by diffraction methods, charge and spin densities being given by X-ray and polarized neutron diffraction (PND) respectively. Our PND studies on the M^{II} ammonium Tutton salts (M = V, Cr, Mn, Fe and Ni) have shown the extent of σ and π metal–water bonding, electron correlation effects, and spin-orbit coupling effects (Fender, Figgis, Forsyth, Reynolds & Stevens, 1986; Fender, Figgis & Forsyth, 1986; Deeth, Figgis, Forsyth, Kucharski & Reynolds, 1989; Figgis, Forsyth, Kucharski, Reynolds & Tasset, 1989; Delfs, Figgis, Forsyth, Kucharski, Reynolds & Vrtis, 1991). A complementary charge-density study on the Cr^{II} salt also showed charge effects associated with the Jahn–Teller distortion around the Cr^{II} centre and different covalence of the long and short Cr–water bonds (Figgis, Kucharski & Reynolds, 1990). X-ray diffraction film methods have been used to investigate ammonium Tutton salts by Montgomery & Lingafelter (1966) and Webb, Kay & Grimes (1965), while single-crystal neutron diffraction studies at room temperature have been used by Brown & Chidambaram (1969) and Maslen, Watson & Moore (1988) to investigate the copper salts.

In this paper we present a charge density study of the deuterated Cu^{II} ammonium Tutton salt. As well as the effects observed in the Cr^{II} case, although in different balance due to changes in $3d$ population and covalence, here we may expect added complications due to the more irregular environment around Cu^{II}.

This Cu^{II} salt has been extensively studied by other means. At higher temperatures the hexaaquacopper(II) ion is in a state of dynamical structural flux (Riley, Hitchman & Mohammed, 1987; and references cited therein), so only low-temperature data where a single structural configuration is frozen out are useful in defining the bonding. At low temperatures the hydrogeneous salt, on which almost all experiments have been carried out, occupies a different minimum, with Cu—O(7) the long bond (Alcock, Duggan, Murray, Tyagi, Hathaway & Hewat, 1984), than the deuterated form in which Cu—O(8) is long (Hathaway & Hewat, 1984). Nevertheless we can carry over qualitative conclusions from the H salt to the D salt. We use the D salt here for experimental reasons. There is less incoherent scattering for neutrons and lower thermal motion for X-rays.

ESR, NMR and optical spectra on the compound give information on bonding and the Cu^{II} electronic configuration. The optical spectrum shows a large tetragonal and smaller, but noticeable, rhombic distortion from octahedral symmetry. This can be simply interpreted by angular overlap methods if both σ and π bonding are included (Hitchman & Waite, 1976). ^{17}O NMR shows spin on the oxygen atoms (Poupko & Luz, 1972). The ^{17}O superhyperfine tensor (in Cu doped into the Zn salt), shows spin on the four short-bonded oxygens only, and not in equal quantities in each pair (Getz & Silver, 1974), indicating different covalence to the symmetry unrelated pairs with spin mainly in $3d_{x^2-y^2}$. Furthermore the spin on the O atoms is in $2s/p$ hybrid orbitals. The principal ESR g values are aligned with the Cu—O axes to within 2°. This precludes a large admixture of t_{2g} into the e_g orbitals (Mabbs & Porter, 1974), but the g-tensor symmetry is D_{2h} not D_{4h}. The ^{63}Cu hyperfine coupling tensor also shows D_{2h} symmetry (Bleaney, Bowers & Ingram, 1955; Bleaney, Bowers & Pryce, 1955). ESR values correlate well with the Cu—O bond lengths, indicating that the tetragonal distortion is large and the rhombic one smaller (Waite & Hitchman, 1976).

We thus expect for the deuterated salt case a spin hole in $3d_{x^2-y^2}$ [Cu—O(8) the long bond $//z$], with some admixture of $3d_{z^2}$, due to differences in Cu—O(7) and Cu—O(9) bond lengths (Hathaway & Hewat, 1984), which give a tetragonal distortion with some rhombic component. This picture may be modified by covalent spin and charge transfers.

Experimental

A pale-blue transparent deuterated (>98%) crystal, prepared by repeated recrystallization from D_2O, of dimensions 0.204 ($\bar{1}10$ to $1\bar{1}0$), 0.380 ($20\bar{1}$ to $\bar{2}01$), 0.380 (110 to $\bar{1}\bar{1}0$), 0.38[illegible] ($01\bar{1}$ to $0\bar{1}1$) and 0.290 mm (001 to $00\bar{1}$) was mounted on a Syntex $P2_1$ diffractometer with a locally developed low-temperature nitrogen gas-flow accessory operating at 85 (2) K. Graphite-monochromatized Mo $K\alpha$ radiation was employed. The unit cell was determined by least-squares fitting of the setting angles of 14 well-spaced reflections with $36 < 2\theta < 39.4°$. A complete sphere of data was collected, with an ω–2θ scan of ω width 1.1° plus $\alpha_1 - \alpha_2$ splitting, to $2\theta = 100°$, followed by a second sphere to 60°. In all, 47 072 reflections were measured. The six standards, measured after every 94 reflections, showed no significant change in intensity over the data-collection period. 3853 reflections with $I/\sigma(I) > 20$ and $I < 80\,000$ counts were used to refine the crystal dimensions so as to maximize the agreement between equivalent reflections after a Gaussian-integration absorption correction using the *XTAL* system (Hall & Stewart, 1990). All data were

then corrected for absorption ($0.572 <$ transmission < 0.733), and reduced by averaging equivalents to 7287 unique reflections with $[(\sin\theta)/\lambda]_{max} = 1.08$ Å^{-1}, $|h| < 20$, $|k| < 27$, $|l| < 12$; R_{int} 0.024.

Refinements

Applying the conclusions of the Cr^{II} experiment we refined a model with anisotropic harmonic temperature factors (deuterium isotropic), quartic isotropic anharmonic thermal parameters on non-D atoms, a charge-density model, and a two-parameter multiple-scattering correction. Extinction, when introduced, was found not to be significant. We used the program *ASRED* (Figgis, Reynolds & Williams, 1980); scattering factors were calculated for core and valence functions from the atomic wavefunctions of Clementi & Roetti (1974) using the program *JCALC* (Figgis, Reynolds & White, 1987), except for D where the function of Stewart, Davidson & Simpson (1965) was used. We applied the anomalous-dispersion correction of Kissel & Pratt (1990) and Cromer & Liberman (1970). All 7287 reflections were refined to minimize the function $\sum[\sigma(I)]^{-2}[I(\text{obs}) - I(\text{calc})]^2$ until a maximum shift/e.s.d. of 0.1 was obtained. Examination of Fourier difference maps showed a large (ρ_{max} *ca* 0.55 e Å^{-3}) anisotropic residual around the Cu^{II} site, but a flat map (< 0.2 e Å^{-3}) everywhere else. Introduction of the full 15-parameter quartic anharmonic thermal parameter set to Cu reduced this substantially, and improved agreement factors by *ca* 0.3%, whereas other *ad hoc* additions to the valence model did neither. The results of this refinement are given in Table 1.

The charge-density model used is a slight modification of the valence model found sufficient to give negligible residuals in the Cr^{II} case. The local-axis systems used were: Cu $z \rightarrow$ O(8), $x \rightarrow$ O(7); S z in the O(3)—S—O(4) plane, $x \rightarrow$ O(4); O(3) to O(6), $x \rightarrow$ S; O(7) to O(9), $x \rightarrow$ Cu, z in the plane defined by Cu—O and the midpoint of the attached D atoms; N, $x \rightarrow$ D(11), z in the D(11)—N—D(12) plane. We placed four sp^3 hybrids on S, N and O(7)—O(9); $2p_\pi$ and two sp hybrids on O(3)—O(6); 1s on the D sites; and seven Gaussian functions of mean-square width 0.16 Å^2 in the midpoints of the S—O and Cu—O bonds. For the sp hybrids $(sp)_1$ points along $+x$, for sp^3 $(sp^3)_1$ along $+x$ and $(sp^3)_2$ in the xz plane.

Because of the expected lowering from tetragonal symmetry in the Cr^{II} salt to something lower in the Cu^{II} case we placed on Cu, besides the core and 4p functions, the six 3d functions allowed in D_{2h} symmetry (xy, xz, yz, z^2, $x^2 - y^2$ and $z^2/x^2 - y^2$ mixing). In addition all heavy-atom valence-function radii were allowed to vary in the manner of the usual κ refinement.

Table 1. *Refinement results*

	Unconstrained	Cu 3d, NH_4, SO_4 symmetry constrained
No. of observations, all data used	7287	7287
Total No. of parameters	228	180
No. of valence parameters	77	29
Multiple-scattering parameters	2	2
$F(000)$	431.7	431.6
Scale factor	11.93 (1)	11.93 (1)
$R(I)$, all data (%)	1.96	2.12
$wR(I)$, all data (%)	2.79	2.86
$R(F)$, only data $I > 3\sigma(I)$ (%)	1.42	1.45
χ, goodness of fit	1.13	1.15

Table 2. *Atomic fractional positional coordinates* ($\times 10^5$, *except for* D, $\times 10^3$) *and equivalent isotropic thermal parameters* (Å$^2 \times 10^4$)

$U_{eq} = (U_{11} + U_{22} + U_{33})/3$.

	x	y	z	U_{eq}
Cu	0	0	0	76
S	38700 (1)	14378 (1)	74928 (2)	65
O(3)	38047 (2)	23885 (2)	60633 (4)	120
O(4)	52770 (3)	08741 (2)	77513 (4)	128
O(5)	26122 (3)	07345 (2)	63017 (4)	105
O(6)	37304 (2)	17335 (2)	97822 (5)	119
O(7)	15161 (3)	10730 (3)	16490 (5)	125
O(8)	−18073 (4)	11191 (2)	05034 (5)	131
O(9)	00960 (3)	−06605 (2)	29598 (4)	111
N	12594 (4)	36442 (3)	37757 (5)	134
D(11)	58 (1)	350 (1)	264 (2)	209
D(12)	190 (1)	317 (1)	413 (1)	191
D(13)	90 (1)	372 (1)	483 (1)	204
D(14)	167 (1)	418 (1)	358 (1)	242
D(15)	192 (1)	94 (1)	304 (2)	43
D(16)	221 (1)	122 (1)	111 (1)	52
D(17)	−264 (1)	104 (1)	−27 (1)	104
D(18)	−164 (1)	173 (1)	34 (1)	78
D(19)	−71 (1)	−66 (1)	321 (1)	57
D(20)	38 (1)	−129 (1)	313 (1)	55

The atomic coordinates and equivalent isotropic thermal parameters are given in Table 2, and the principal interatomic distances and angles in Table 3.*

Deformation and residual density maps based on the refinement were constructed using the refined scale, thermal and positional parameters. We subtracted theoretical structure factors derived from, respectively, theoretical atomic and fitted model atomic form factors from the experimental structure factors. The maps are shown in Figs. 1–5 for the three hexaaquametal-ion planes containing oxygens, and representative sulfate and ammonium planes. A wavevector cutoff of 0.8 Å^{-1} was used. Away from the atomic cores the uncertainty resulting from random stucture-factor errors is less than 0.05 e Å^{-3}.

* Lists of least-squares planes for the $Cu(OD_2)_6^{2+}$ cation, anisotropic thermal parameters, valence parameters and structure factors have been deposited with the British Library Document Supply Centre as Supplementary Publication No. SUP 54679 (29 pp.). Copies may be obtained through The Technical Editor, International Union of Crystallography, 5 Abbey Square, Chester CH1 2HU, England. [CIF reference: AL0504]

Table 3. *Bond lengths* (Å) *and angles* (°)

Cu—O(7)	2.0104 (4)	S—O(3)	1.4755 (3)
Cu—O(8)	2.3013 (5)	S—O(4)	1.4702 (4)
Cu—O(9)	1.9602 (3)	S—O(5)	1.4871 (3)
O(7)—D(15)	0.84 (1)	S—O(6)	1.4822 (4)
O(7)—D(16)	0.83 (1)	N—D(11)	0.81 (1)
O(8)—D(17)	0.80 (1)	N—D(12)	0.83 (1)
O(8)—D(18)	0.81 (1)	N—D(13)	0.81 (1)
O(9)—D(19)	0.82 (1)	N—D(14)	0.80 (1)
O(9)—D(20)	0.84 (1)		

O(7)—Cu—O(8)	92.31 (2)	D(15)—O(7)—D(16)	105.4 (7)
O(7)—Cu—O(9)	90.12 (1)	D(17)—O(8)—D(18)	104.1 (7)
O(8)—Cu—O(9)	91.27 (1)	D(19)—O(9)—D(20)	105.5 (7)
Cu—O(7)—D(15)	114.2 (5)	O(3)—S—O(4)	109.87 (2)
Cu—O(7)—D(16)	118.9 (5)	O(3)—S—O(5)	108.30 (2)
Cu—O(8)—D(17)	119.1 (6)	O(3)—S—O(6)	110.20 (2)
Cu—O(8)—D(18)	113.3 (6)	O(4)—S—O(5)	108.78 (2)
Cu—O(9)—D(19)	111.9 (5)	O(4)—S—O(6)	110.37 (1)
Cu—O(9)—D(20)	116.2 (5)	O(5)—S—O(6)	109.29 (2)

Hydrogen bonds

D(15)—O(5)	1.91 (1)	D(20)—O(3)	1.84 (1)
D(16)—O(6)	1.95 (1)	D(11)—O(6)	2.08 (1)
D(17)—O(4)	1.98 (1)	D(12)—O(3)	2.08 (1)
D(18)—O(6)	2.02 (1)	D(13)—O(4)	2.09 (1)
D(19)—O(5)	1.90 (1)	D(14)—O(5)	2.08 (1)

D(11)—N—D(12)	112.5 (7)	O(8)—D(17)—O(4)	178.8 (8)
D(11)—N—D(13)	107.2 (9)	O(8)—D(18)—O(6)	177.4 (7)
D(11)—N—D(14)	110.4 (7)	O(9)—D(19)—O(5)	176.3 (7)
D(12)—N—D(13)	109.0 (7)	O(9)—D(20)—O(3)	171.2 (7)
D(12)—N—D(14)	107.9 (8)	N—D(11)—O(6)	174.3 (8)
D(13)—N—D(14)	109.8 (7)	N—D(12)—O(3)	157.5 (7)
O(7)—D(15)—O(5)	171.7 (8)	N—D(13)—O(4)	170.0 (6)
O(7)—D(16)—O(6)	173.4 (7)	N—D(14)—O(5)	163.3 (7)

This is less than other systematic errors and is not discussed further.

We also performed a refinement in which the valence parameters were constrained to idealized local symmetries, copper to D_{4h}, sulfate and ammonium to tetrahedral T_d. The resulting fit is given in Table 1, and values for the valence parameters and resulting charges in Tables 4 and 5. The degradation in fit is almost entirely due to sulfate and ammonium constraints.

Except for obvious differences such as 3*d* populations, the fits and parameter values bear a striking resemblance to those for the Cr^{II} salt. We therefore do not discuss other refinements involving spherical theoretical form factors, spherical valence form factors, harmonic motion *etc.*, which were conducted, merely noting that changes in agreement factors and other parameters follow those for the Cr^{II} salt described fully by Figgis *et al.* (1990).

Table 4. *Valence parameters obtained from the refinement constrained to D_{4h} symmetry, rescaled to the theoretical total electron count*

	Valence parameters				
Cu	$3d_{xy}$ 1.58 (6)	$3d_{xz}$ 2.12 (3)	$3d_{yz}$ $=3d_{xz}$	$3d_{x^2-y^2}$ 0.82 (7)	$3d_{z^2}$ 2.18 (6)
	$4p_x$ −0.19 (10)	$4p_y$ $=4p_x$	$4p_z$ 0.22 (17)	κ_{3d} 1.03 (1)	
S	$(sp^3)_1$ 0.81 (2)	$(sp^3)_2$ $=(sp^3)_1$	$(sp^3)_3$ $=(sp^3)_1$	$(sp^3)_4$ $=(sp^3)_1$	κ_{3sp} 0.94 (1)
O(3),O(4) O(5),O(6)	$2p_\pi$ 3.57 (2)	$(sp^1)_1$ 1.27 (2)	$(sp^1)_2$ 1.58 (1)	κ_{2sp} 1.046 (2)	
O(7),O(9)	$(sp^3)_1$ 1.64 (1)	$(sp^3)_2$ 1.52 (2)	$(sp^3)_3$ 1.66 (1)	$(sp^3)_4$ $=(sp_3)_3$	κ_{2sp} 1.033 (2)
O(8)	$(sp^3)_1$ 1.70 (2)	$(sp^3)_2$ 1.50 (2)	$(sp^3)_3$ 1.64 (2)	$(sp^3)_4$ $=(sp^3)_3$	κ_{2sp} 1.038 (3)
N(1)	$(sp^3)_1$ 1.01 (3)	$(sp^3)_2$ $=(sp^3)_1$	$(sp^3)_3$ $=(sp^3)_1$	$(sp^3)_4$ $=(sp^3)_1$	κ_{2sp} 0.90 (2)
D(11),D(12) D(13),D(14)	(1*s*) 1.08 (3)		D(15),D(16) D(19),D(20)	(1*s*) 0.72 (1)	
D(17),D(18)	(1*s*) 0.73 (2)				
X(3),*X*(4) *X*(5),*X*(6)	Population 0.64 (2)		*X*(7),*X*(9)	Population 0.24 (2)	
X(8)	Population 0.04 (3)				

Table 5. *Charges obtained from the constrained refinement, rescaled to neutral crystal, and those obtained from Cr^{II} data*

	Cr refinement	This Cu data
Cr/Cu 3*d* population	4.45 (7)	8.83 (13)
4*p* population	0.07 (21)	−0.15 (26)
Total charge	+1.19 (22)	+1.81 (26)
O(7,9)	−0.71 (3)	−0.61 (3)
O(8)	−0.47 (4)	−0.50 (4)
D(15,16,19,20)	+0.35 (1)	+0.28 (1)
D(17,18)	+0.24 (1)	+0.27 (1)
O(7,9)D_2	−0.00 (4)	−0.04 (4)
O(8)D_2	+0.02 (4)	+0.05 (4)
Cr/Cu$(OD_2)_6$	+1.21 (17)	+1.74 (20)
S	+1.94 (8)	+1.47 (9)
O(3–6)	−0.82 (3)	−0.75 (3)
SO_4	−1.33 (13)	−1.53 (14)
N	+0.98 (14)	+0.96 (13)
D(11–14)	−0.06 (4)	−0.08 (3)
ND_4	+0.74 (16)	+0.63 (15)

Discussion

Geometry and thermal motion

The hydrogen-bonding network is similar to that in the Cr^{II} and other ammonium Tutton salts.

It is interesting to compare the sulfate-ion geometry to that observed in the Cr salt. In neither is it quite of ideal tetrahedral symmetry, and the distortions are very similar. The powder neutron diffraction results are not sufficiently precise to warrant comparison.

The Jahn–Teller distortion of the hexaaqua ion measured here agrees well with the neutron results of Hathaway & Hewat (1984), corresponding to a 0.32 Å lengthening of Cu—O(8) with a slight rhombic distortion of 0.025 Å in the Cu—O(7)—O(9) plane. Their results also show that at 85 K in the deuterated salt (but not the hydrogeneous one) we can neglect any populations of the alternate minimum reached by shortening Cu—O(8) and

lengthening Cu—O(7). While the harmonic thermal parameters show no obvious effects of this fluxional possibility, the anharmonic parameters on the copper do. If we do not include the anharmonic parameters on Cu we see an excess charge density in the deformation density almost in the Cu—O(7)—O(8) plane, and a deficit in the Cu—O(9) direction. This anisotropy is explicable in terms of a potential anharmonically softening in the Cu—O(7)—O(8) plane compared to the other vibrational coordinates. Since motions in this plane are just those required to surmount the potential barrier into the alternate minimum, and the barrier is thermally accessible at higher temperatures, this softening is readily accounted for. We note that in the Cr^{II} salt the energy difference between minima is larger, and so presumably is the barrier height, and no comparable observed anisotropic anharmonicity is observed in that case.

Deformation density maps

As with the Cr^{II} experiment, where it is discussed in more detail, we can see a number of qualitative features in the deformation density maps (Figs. 1*a*–5*a*).

(1) A peak on Cu corresponding to a net charge gain; with a deficit in the Cu—O(7) and Cu—O(9) directions, corresponding to a depopulation of $3d_{x^2-y^2}$ compared to a spherical ion.

(2) Lone-pair peaks on the water oxygen atoms, pointed at the Cu atom. The O(8) peak is less extended in space and higher than the other two, suggesting less covalence to O(8).

(3) The sulfate ion appears to retain the tetrahedral symmetry of the free ion in the deformation density. We see a density very similar to that in the Cr salt – a mid S—O bond peak of 0.7 e $Å^{-3}$, a lone-pair region on the far side of the S—O bonds, and a negative region around S at *ca* 0.9 Å, except along the S—O bonds.

The residual-density maps (Figs. 1*b*–5*b*) show negligible density, except around Cu. There residuals of up to 0.2 e $Å^{-3}$ are present. They are greater than for the Cr case, probably reflecting both the greater number of 3*d* electrons and the much increased anharmonicity.

Population analysis

The low goodness-of-fit, and generally small residuals, imply that our model in which the charge density of each atom fragment is adapted to its local symmetry is appropriate.

The charges on the major fragments are, as with the Cr^{II} salt, reduced compared with free-ion values (Table 5). Again we refer to the appropriate paper (Figgis *et al.*, 1990) for a discussion of the meaning of these values. The sulfate-ion charge is slightly, but not significantly, more negative than for the Cr^{II} case [−1.53 (14) *versus* −1.33 (13)]. Similarly, the ammonium ion may be less positive [+0.63 (15) *versus* +0.74 (16)]. This is the result of a significant difference in the hexaaqua-ion charges [+1.74 (20) *versus* +1.21 (17)]. The $Cu(OD_2)_6$ ion has far less charge transferred to it than the Cr ion. The water molecule charges are similar, the difference resides at the metal site, reflecting differences in the covalent behaviour of the metal–water bonds which we discuss later.

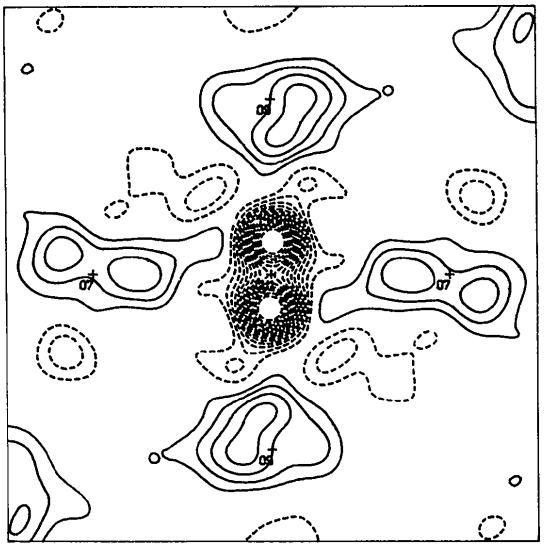

(*a*)

(*b*)

Fig. 1. (*a*) Deformation density in the $Cu(OD_2)_6$ fragment. Cu—O(7)—O(9) plane. Contour interval 0.1 e $Å^{-3}$: positive solid, negative dotted, zero suppressed. Box size 5.98 × 5.98 Å. (*b*) Residual density in the $Cu(OD_2)_6$ fragment. Cu—O(7)—O(9) plane.

The water molecules remain almost neutral, the charge transferred to metal being balanced by charge gained from hydrogen bonding from the sulfate ion. The O(7) and O(9) waters are more electrically polarized than the O(8) water, but the effect is less marked than for the Cr^{II} case.

To discuss the Cu water bonding we use the tetragonal refinement results, except where an explicit consideration of rhombic distortion is required. For a Jahn–Teller-distorted crystal-field-perturbed Cu^{2+} ion we expect all $3d$ orbitals to have a population of 2 except $3d_{x^2-y^2}$ with one electron. Except for the low $3d_{xy}$ population this is approximately as observed (Table 4). It is possible that the low $3d_{xy}$ population is due to signficant π back donation onto the O(7,9) waters. However, given the anharmonicity present, we cannot be sure of this. The $3d_{x^2-y^2}$ orbital has not gained any significant population by σ transfer. If we ascribe half the total Cu—O overlap density to σ bonding we find for Cu, totalling all populations of σ symmetry, a σ gain of 0.52 (10) and a π back donation of 0.18 (10) e. For the Cr case the corresponding σ acceptance is 0.46 (6) and π *acceptance* is 0.30 (5). The net result of the π back donation, as opposed to π donation for Cr, together with comparable σ-bonding trans-

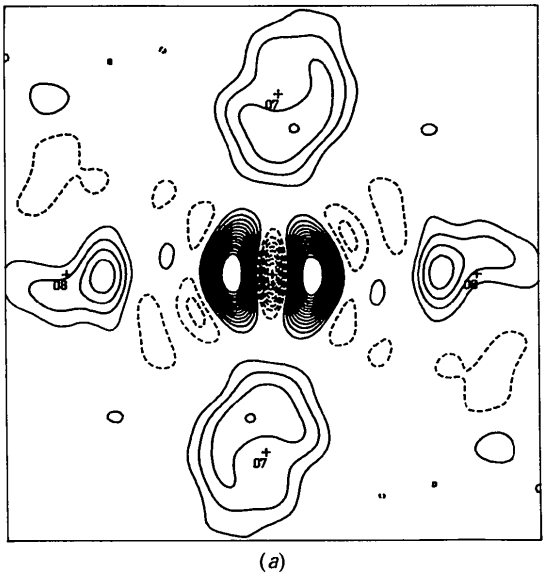

(*a*)

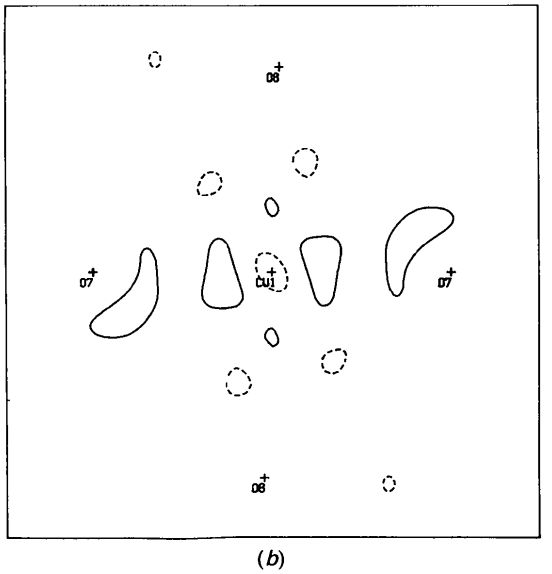

(*b*)

Fig. 2. (*a*) Deformation density in the $Cu(OD_2)_6$ fragment. Cu—O(7)—O(8) plane. (*b*) Residual density in the $Cu(OD_2)_6$ fragment. Cu—O(7)—O(8) plane.

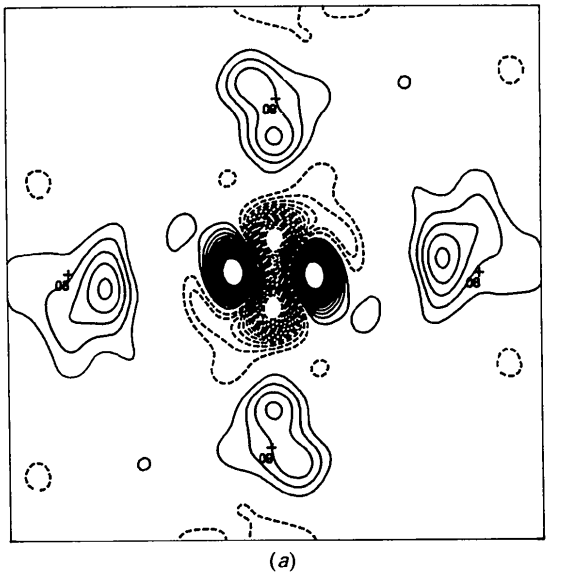

(*a*)

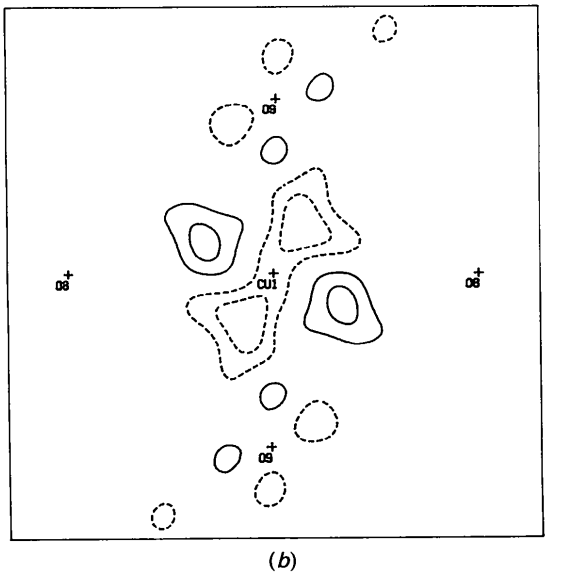

(*b*)

Fig. 3. (*a*) Deformation density in the $Cu(OD_2)_6$ fragment. Cu—O(8)—O(9) plane. (*b*) Residual density in the $Cu(OD_2)_6$ fragment. Cu—O(8)—O(9) plane.

fers, is the smaller positive charge on Cr than Cu. We should not take the division into σ and π effects too literally since, apart from any difficulty with Mulliken charge partitioning, and the lack of ligand symmetry required for exact σ/π separation, we also assume common radial dependences for 'σ' and 'π' atomic components of the molecular orbitals. This may be a significant approximation.

The smaller charge transfers within the hexaaqua ions, and the smaller polarization of the water molecules, implies weaker metal–water bonding for Cu than for Cr. This agrees with the experimental heats of ion hydration [332 kJ mol^{-1} for Cr^{2+} compared with 81 kJ mol^{-1} for Cu^{2+} (Benjamin & Gold, 1954)], but *a priori* we would have expected more σ covalence for the Cu ion than the Cr. A polarized neutron diffraction study of the magnetization distribution would elucidate this, since it focusses on the bonding unpaired spin. Such a study is available for the Cr^{II} salt (Delfs *et al.*, 1991).

The rhombic distortion allows the $3d_{z^2}$ orbital to mix with the $3d_{x^2-y^2}$ orbital. For a small mixing coefficient the amount of 'hole' transferred from $3d_{x^2-y^2}$ to $3d_{z^2}$ will be unobservably small. However, the $3d_{z^2}/3d_{x^2-y^2}$ mixing term may not be. We observe a value of -0.34 (11) e. This is of the expected sign,

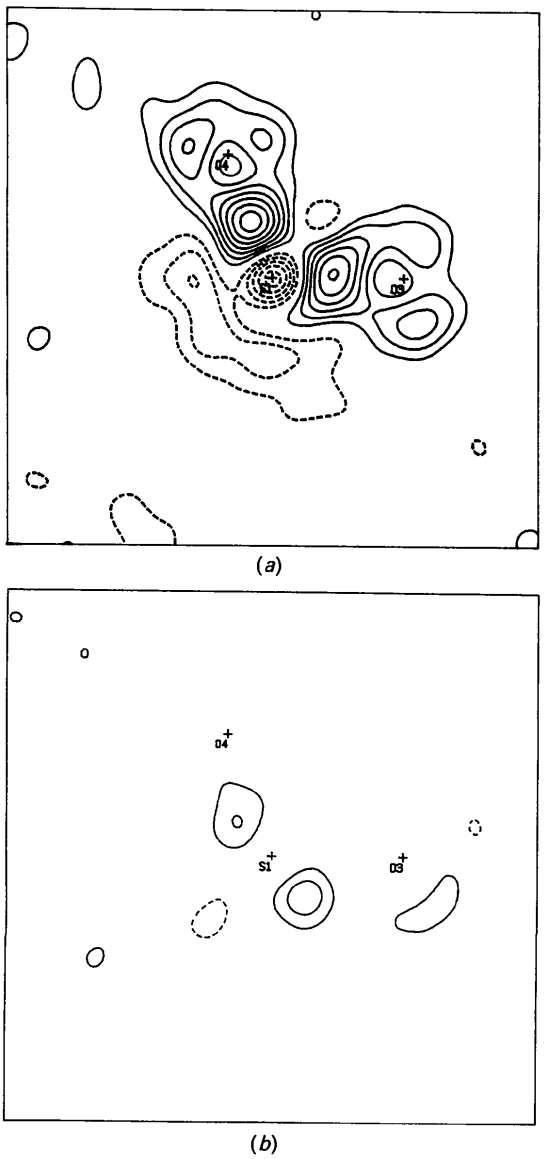

Fig. 4. (*a*) Deformation density in the SO_4 fragment. S—O(3)—O(4) plane. (*b*) Residual density in the SO_4 fragment. S—O(3)—O(4) plane.

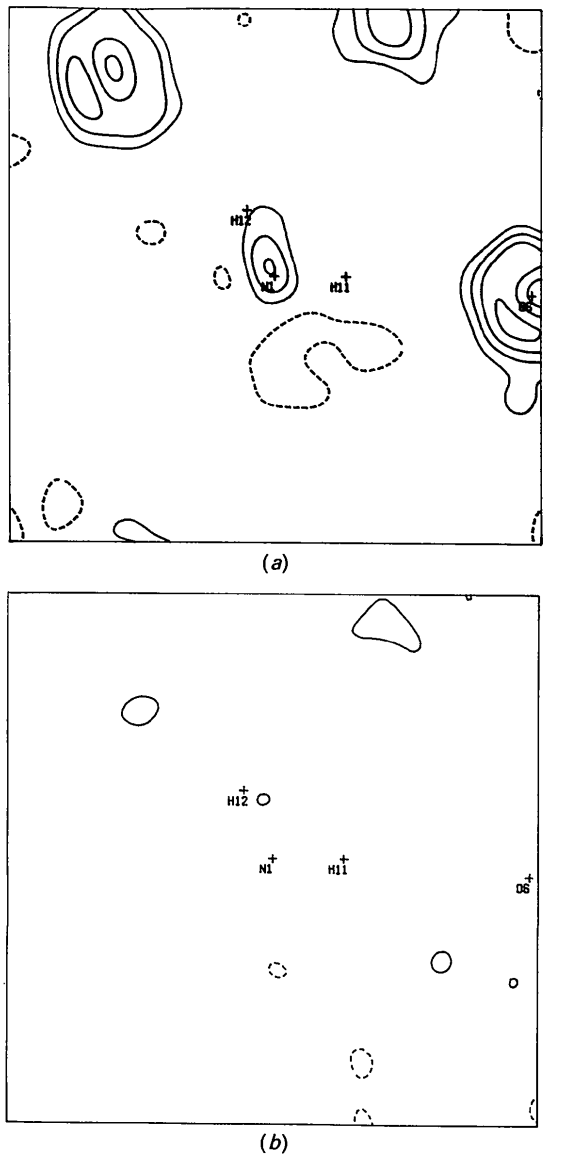

Fig. 5. (*a*) Deformation density in the ND_4 fragment. N—D(11)—D(12) plane. (*b*) Residual density in the ND_4 fragment. N—D(11)—D(12) plane.

removing charge density from the shortest Cu—O(9) bond. It corresponds to a $\langle 3d_{z^2}\rangle$ coefficient of -0.21 (7). At room temperature Waite & Hitchman (1976) found a coefficient from the ESR g value of -0.15 (1). This may not be directly comparable with the present case since it is for the hydrogenous salt at room temperature. However, they found that a range of Tutton salts also give negative coefficients of about this magnitude.

Concluding remarks

The electronic charge distribution in the $3d^9$ $Cu(OD_2)_6$ ion in ammonium cupric Tutton salt strongly reflects the large Jahn–Teller effect present. The results resemble those found earlier for the $3d^4$ Cr^{II} case, which is also strongly Jahn–Teller sensitive. The charge flow and the overlap density concerned with the longer Cu—O(8) bond are markedly less than for the shorter such bonds in the plane perpendicular to it. These observations again demonstrate the expected strong dependence of covalent character on bond length, also seen in the Cr^{II} salt.

The copper atom $3d$ and $4p$ populations depart strongly from cubic symmetry, and do so in the manner expected from simple crystal-field arguments, with the lowest value being in the $3d_{x^2-y^2}$ orbital. However, covalence effects act to reduce the populations of the other $3d$ orbitals, except for the $3d_{z^2}$ orbital which is directed along the Cu—O(8) bond, but to an extent rather less than for the Cr^{II} case.

The ammonium and sulfate ions are close in shape to their idealized tetrahedral symmetry with, as is commonly observed, effective charges somewhat lower than the formal values of $1+$ and $2-$.

The thermal motion appears to contain an appreciable anharmonic component, and this reduces the reliability of the above deductions relative to some other low-temperature charge-density studies on transitional-metal complexes (Reynolds & Figgis, 1990).

The authors are grateful to the Australian Research Council for financial support and to the University of Western Australia Crystallography Centre for access to the diffractometer.

References

ALCOCK, N. W., DUGGAN, M., MURRAY, A., TYAGI, S., HATHAWAY, B. J. & HEWAT, A. (1984). *J. Chem. Soc. Dalton Trans.* pp. 7–14.

BENJAMIN, L. & GOLD, V. (1954). *Trans. Faraday Soc.* **50**, 797–799.

BLEANEY, B., BOWERS, K. D. & INGRAM, D. J. E. (1955). *Proc. R. Soc. London Ser. A*, **224**, 147–155.

BLEANEY, B., BOWERS, K. D. & PRYCE, M. L. H. (1955). *Proc. R. Soc. London Ser. A.* **228**, 166–174.

BROWN, G. M. & CHIDAMBARAM, R. (1969). *Acta Cryst.* B**25**, 676–687.

CLEMENTI, E. & ROETTI, C. (1974). *At. Data Nucl. Data Tables*, **14**, 177–478.

CROMER, D. T. & LIBERMAN, D. (1970). *J. Chem. Phys.* **53**, 1891–1898.

DEETH, R. J., FIGGIS, B. N., FORSYTH, J. B., KUCHARSKI, E. S. & REYNOLDS, P. A. (1989). *Proc. R. Soc. London Ser. A*, **421**, 153–168.

DELFS, C. D., FIGGIS, B. N., FORSYTH, J. B.. KUCHARSKI, E. S., REYNOLDS, P. A. & VRTIS, M. (1991). *Proc. R. Soc. London Ser. A*. In the press.

FENDER, B. E. F., FIGGIS, B. N. & FORSYTH, J. B. (1986). *Proc. R. Soc. London Ser. A*, **404**, 139–145.

FENDER, B. E. F., FIGGIS, B. N., FORSYTH, J. B., REYNOLDS, R. A. & STEVENS, E. (1986). *Proc. R. Soc. London. Ser. A*, **404**, 127–138.

FIGGIS, B. N., FORSYTH, J. B., KUCHARSKI, E. S., REYNOLDS, P. A. & TASSET, F. (1989). *Proc. R. Soc. London Ser. A*, **428**, 113–124.

FIGGIS, B. N., KUCHARSKI, E. S. & REYNOLDS, P. A. (1990). *Acta Cryst.* B**46**, 577–586.

FIGGIS, B. N., REYNOLDS, P. A. & WHITE, A. H. (1987). *J. Chem. Soc. Dalton Trans.* pp. 1737–1745.

FIGGIS, B. N., REYNOLDS, P. A. & WILLIAMS, G. A. (1980). *J. Chem. Soc. Dalton Trans.* pp. 2339–2347.

GETZ, D. & SILVER, B. L. (1974). *J. Chem. Phys.* **61**, 630–637.

HALL, S. R. & STEWART, J. M. (1990). Editors. *XTAL3.0 Users Manual.* Univs. of Western Australia, Australia, and Maryland, USA.

HATHAWAY, B. J. & HEWAT, A. W. (1984). *J. Solid State Chem.* **51** 364–375.

HITCHMAN, M. A. & WAITE, T. D. (1976). *Inorg. Chem.* **15**, 2150–2154.

KISSEL, L. & PRATT, R. H. (1990). *Acta Cryst.* A**46**, 170–175.

MABBS, F. E. & PORTER, J. K. (1973). *J. Inorg. Nucl. Chem.* **35**, 3219–3222.

MASLEN, E. N., WATSON, K. J. & MOORE, F. H. (1988). *Acta Cryst.* B**44**, 102–107.

MONTGOMERY, H. & LINGAFELTER, E. C. (1966). *Acta Cryst.* **20**, 659–662.

POUPKO, R. & LUZ, Z. (1972). *J. Chem. Phys.* **57**, 3311–3318.

REYNOLDS, P. A. & FIGGIS, B. N. (1990). *Aust. J. Chem.* **43**, 1929–1934.

RILEY, M. J., HITCHMAN, M. A. & MOHAMMED, A. W. (1987). *J. Chem. Phys.* **87**, 3766–3778.

STEWART, R. F., DAVIDSON, E. R. & SIMPSON, W. T. (1965). *J. Chem. Phys.* **42**, 3175–3187.

WAITE, T. D. & HITCHMAN, M. A. (1976). *Inorg. Chem.* **15**, 2155–2158.

WEBB, M. W., KAY, H. F. & GRIMES, N. W. (1965). *Acta Cryst.* **18**, 740–742.